Impact Theory of the Noble-Gas-Broadened HCl Vibration-Rotation Lines*

ROGER M. HERMAN†
Yale University, New Haven, Connecticut‡
(Received 24 May 1963)

The widths and shifts of the noble-gas-broadened HCl (0–1) and (0–2) band vibration-rotation lines are calculated using an impact theory similar to Anderson's. To obtain agreement with the experimentally observed shifts, Anderson's approach is modified in that the imaginary parts of the optical cross sections are calculated in greater detail. The cross sections are evaluated in a representation which allows further understanding of the physical processes active in impact broadening. It is shown that many broadening and shifting characteristics can be explained upon taking into account the eccentricity of the HCl molecule, in which the centers of charge and mass do not coincide. Substantial agreement with experiment is reached, although several features of the observed shapes and shifts—particularly the variation in width with perturber species—remain unexplained.

I. INTRODUCTION

In recent years, many advances in near infrared spectroscopy (1–5 μ) have been made.[1] Presently, the rotational fine structure of many molecular vibrational bands can be resolved with ease. In some cases, investigators have examined the finer details of these spectra in an effort to gain fundamental information not only about the molecules themselves, but also about the way in which these molecules interact with each other and with foreign gases. Considerable experimental effort has been spent, for example, on observations of pressure broadening and shifting in the vibration-rotation spectra of polar diatomic molecules, particularly the hydrogen halides.[2–10]

The molecule whose spectrum appears to have been most fully examined is HCl. It is to the problem of interpreting the observed shapes and shifts of the HCl (0–1) and (0–2) band absorption-lines broadened by noble gases that the present paper is addressed. In comparing theory with experiment, we draw freely on experimental results reported in Refs. 4, 7, and 10. The restriction to noble gases is made because the structure of these gases is less complicated than that of other foreign gases used in experimental studies, inasmuch as the rare gases are chemically inert and possess no unpaired angular momenta nor permanent moments. Correspondingly, molecular interactions involving these gases should be relatively simple.

Observations reveal that the rare-gas-broadened lines have the following reasonably regular features:

(1) The lines are Lorentz-shaped, at least near their centers.

(2) The line-shape parameters are strongly dependent upon the rotational quantum numbers of the states between which the radiative transitions occur. Some features of the shifts' and widths' m dependence appear to be the same for all rare-gas broadeners. These are: (a) The widths are greatest for the low $|m|$ lines, diminishing as $|m|$ becomes successively larger. (b) The changes in width from one line to another become smaller as $|m|$ increases. (c) The m dependence of the shifts appears to be correlated with that of the widths. In some cases, the shifts tend to level off at higher values of $|m|$, as do the widths. (d) The widths appear to be independent of the sign of m.

(3) The widths and shifts also vary with the vibrational quantum number of the upper state. Specifically, (a) The shifts of the (0–2) band lines are roughly twice those of the (0–1) band lines, especially for high $|m|$ values. (b) The widths of the (0–2) band are also somewhat greater than those of the (0–1) band lines, especially for high $|m|$.

The present calculations lead to modest agreement with experiment. The greatest single discrepancy lies in the fact that the variation in the experimentally observed widths and shifts in going from one foreign gas to another is not explained satisfactorily. Specifically, the predicted widths for neon- and helium-broadened lines are two to three times those which have been

---

* Part of a dissertation presented to the faculty of the Graduate School of Yale University in candidacy for the degree of Doctor of Philosophy. Presented in part at the symposium on "Quantitative Spectroscopy and Applications in Space Science," Pasadena, California, 1963. Research supported in part by the Office of Naval Research.

† Loomis Fellow, 1961–62.

‡ Present address: Space Technology Laboratories, Inc., Redondo Beach, California.

[1] Recent progress in this field has been reviewed, briefly, by D. H. Rank, Rev. Mod. Phys. **34**, 577 (1962).

[2] W. S. Benedict, R. Herman, G. E. Moore, and S. Silverman, Can. J. Phys. **34**, 850 (1956).

[3] D. F. Smith, presented at the conference on Molecular Interactions and Spectral Line Shape, Weizmann Institute of Science, Rehovot, Israel, 1961 (unpublished); W. F. Herget, W. E. Deeds, N. M. Gailar, R. J. Lovell, and A. H. Nielsen, J. Opt. Soc. Am. **52**, 1113 (1962).

[4] H. Babrov, G. Ameer, and W. Benesch, J. Chem. Phys. **33**, 145 (1960).

[5] G. Ameer and W. Benesch, J. Chem. Phys. **37**, 2699 (1962).

[6] S. Kimel, M. A. Hirshfeld, and J. H. Jaffe, J. Chem. Phys. **31**, 81 (1959).

[7] A. Ben-Reuven, S. Kimel, M. A. Hirshfeld, and J. H. Jaffe, J. Chem. Phys. **35**, 955 (1961).

[8] J. A. Jaffe, A. Landau, and A. Ben-Reuven, J. Chem. Phys. **36**, 1946 (1962).

[9] D. H. Rank, D. P. Eastman, W. B. Birtley, and T. A. Wiggins, J. Chem. Phys. **33**, 323 and 327 (1960).

[10] D. H. Rank, D. P. Eastman, B. S. Rao, and T. A. Wiggins, presented at the symposium on Effects on Intermolecular Forces on Intramolecular Properties, University of Toronto, 1962 (unpublished).

observed, while in krypton and xenon broadening, the predicted widths are somewhat smaller. There are corresponding discrepancies in the predicted and observed shifts for these gases, although these do not appear to be so severe.

The impact approximation, employed in this paper, amounts to considering that impacts occur instantaneously in time. Actually, therefore, the absorbed wave train is replaced by an approximate one which is exact between collisions, while differing markedly from the exact during impacts. Accordingly, all but a fraction $\tau_d\nu_c$ (where τ_d is the duration of typical impacts and ν_c the mean collision frequency) of the radiation amplitude will eventually be Fourier analyzed without approximation. The impact approximation, therefore, leads to calculated line shapes accurate to within a factor $\tau_d\nu_c$ which, in the experiments of interest here ($\approx$STP conditions), is $\approx 1\%$.

Impact theories have already been employed in calculating the widths and shifts of the rare-gas-broadened HCl lines. A calculation by Babrov *et al.*[4] revealed that with their understanding of the long-range forces between argon and HCl, the widths calculated through Anderson's theory did not show good agreement with experiment. Ben-Reuven, Kimel, Hirshfeld, and Jaffe,[7] have made the phase shift approximation in employing an impact theory to obtain m-independent estimates of the shifts which show partial agreement with the argon, krypton, and xenon induced shifts at high $|m|$ values, while Schuller and Oksengorn[11] and Ben-Reuven, Friedmann, and Jaffe[12] have used the same basic approach, with refinements, to obtain m-dependent shifts of the argon- and krypton-broadened lines. Here, again, partial agreement with the observed shifts has been reached.

In this paper, an impact theory in which we have incorporated two innovations is adopted, allowing us to reach closer agreement with experiment than has previously been attained. The first of these arises from our re-examinaton of the forces between polar and spherical molecules to find that the long-range interaction energy has, in fact, a form quite different from that previously considered. Using our modified interaction, the Anderson theory[13,14] can be employed to yield reasonably good agreement between the theoretical and observed widths, at least for the heavier broadeners.

The second change comes in searching for a more complete explanation of the m-dependent shifts than Anderson's theory yields. An alternate approach is taken in which we employ the adiabatic representation (not to be confused with the adiabatic approximation) to evaluate the optical cross sections for broadening and shifting. The terms appearing in the final expressions for optical cross-section contributions arising from collisions having large impact parameter can then be related directly to the phase shift, inelastic, and rotational phenomena associated with molecular scattering. Accordingly, these expressions appear to be more sensible, physically, than analogous ones obtained through the use of the Heisenberg representation. The optical cross sections for shifting are found to differ numerically from those obtained through Anderson's theory, for reasons to be discussed in Sec. IIID. When the shifts are calculated according to the present treatment, the observed m dependencies receive an explanation.

II. THE INTERACTION BETWEEN POLAR AND SPHERICAL MOLECULES

The long-range energy of interaction between polar and spherical molecules is customarily written[7,11]

$$H_{\text{coll}}(1,2;t)=-\frac{(C(v)+\alpha_2\mu^2)}{R(t)^6}-\frac{(\alpha_2\mu^2-\gamma C(v))}{R(t)^6}P_2(\cos\theta)\,, \quad (1)$$

where we have neglected terms higher than inverse sixth power in the intermolecular separation, $R(t)$. The first term represents the isotropic portion of the London dispersion force between the molecules, and is parametrically dependent on the HCl vibrational quantum number. The terms in $\alpha_2\mu^2$ represent the dipole-induced dipole energy (the HCl permanent dipole moment is μ; the perturber polarizability, α_2), while the $\gamma C(v)$ term is a contribution to the dispersion force resulting from the anisotropy of the HCl polarizability. Here,

$$\gamma=(\alpha_{11}-\alpha_1)/(\alpha_{11}+2\alpha_1)\,, \quad (2)$$

α_{11} and α_1 being the components of the polarizability tensor in the direction of, and perpendicular, to the HCl symmetry axis. The latter two terms in Eq. (1) have second-order Legendre-polynomial symmetry.

Now Eq. (1) is true only in the following sense: The $R(t)$ and θ which enter the expression for H_{coll} must be regarded as the distance separating the centers between which the intermolecular attraction takes place, and the angle formed by this line with the HCl figure axis. These centers are nearly coincident with the charge center of the polarizable electrons in each molecule. In the noble gases, the latter coincides with the center of mass while, on the other hand, in HCl such a coincidence is unexpected. Here the bonding electrons, which are highly polarizable, are shared roughly equally by both nuclei, whereas the center of mass nearly coincides with the Cl nucleus. Accordingly, d, the distance separating the center of (dispersion) force and center of mass in HCl

[11] F. Schuller and B. Oksengorn, Mol. Phys. **5**, 573 (1962).
[12] A. Ben-Reuven, H. Friedmann, and J. H. Jaffe, J. Chem. Phys. **38**, 3021 (1963).
[13] P. W. Anderson, Phys. Rev. **76**, 647 (1949).
[14] C. J. Tsao and B. Curnutte, J. Quant. Spectr. Radiative Transfer **2**, 41 (1962).

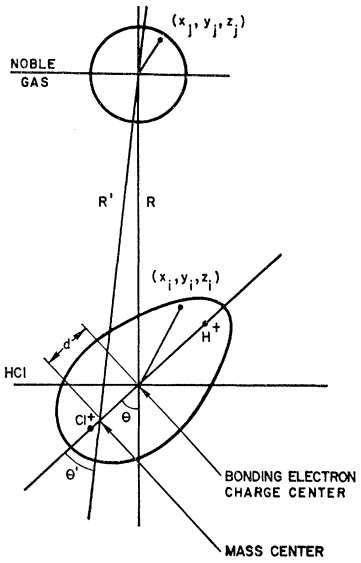

FIG. 1. The HCl-noble-gas binary system.

is of the order of $\frac{1}{2}r_e$, r_e being the equilibrium separation between the H and Cl nuclei. (In HCl, $r_e=1.28$ Å.)

The equations governing the motion of the HCl molecule, on the other hand, are to be written and solved in a coordinate system whose origin coincides with the dynamical center (center of mass) of the molecule, the intermolecular separation being the displacement between mass centers of the emitter and perturber. Accordingly, neglecting all but the first term of Eq. (1), we obtain a Legendre polynomial series for $H_{\text{coll}}(1,2;t)$ in $R'(t)$ and θ'—the center-of-mass coordinates (Fig. 1)—thus:

$$\begin{aligned}H_{\text{coll}}(1,2;t)&=-[C(v)/R'(t)^6]\{(1+5(d/R'(t))^2+\cdots)\\&\quad+(6d/R'(t)+\cdots)P_1(\cos\theta')\\&\quad+(16d^2/R'(t)^2+\cdots)P_2(\cos\theta')+\cdots\}\\&\approx-[C(v)/R'(t)^6]\{1+6(d/R'(t))P_1(\cos\theta')\\&\qquad+16(d/R'(t))^2P_2(\cos\theta')\},\end{aligned}\quad(3)$$

terms or order $[d/R'(t)]^3$ and higher not being shown. The $P_1(\cos\theta')$ term, which is all-important in broadening, results directly from the fact that the dispersion force center is displaced from the mass center in HCl.

Our next step is to calculate the interaction in greater detail. Following the approach taken above, we first calculate in electrical-center coordinates, then transform to the mass-center system. The following definitions prove necessary for the calculation:

$\mathbf{R}$ = vector running from the center of HCl polarizable electronic charge to the noble gas.

$\mathbf{R}'$ = vector running from the HCl center of mass to the noble gas.

θ = angle formed by $\mathbf{R}$ and $\mathbf{r}_{\text{Cl-H}}$, the vector drawn from the Cl to H nucleus.

θ' = angle formed by $\mathbf{R}'$ and $\mathbf{r}_{\text{Cl-H}}$.

$(x_jy_jz_j)$ = coordinates of the jth noble-gas electron in a system of coordinates having its origin at the noble-gas nucleus, and z axis coincident with $\mathbf{R}$.

We assume that the HCl molecule in the electronic ground state consists of a nonpolarizable Cl^+ ion and an H^+ ion bonded together by two shared electrons. Accordingly, $(x_iy_iz_i)$ = coordinates of the ith shared HCl electron in a system of coordinates having its origin at the electrical center of HCl and z axis coincident with $\mathbf{R}$.

$(x_ny_nz_n)$ = coordinates of the nth HCl ion in the same coordinate system.

The HCl figure axis is considered always to lie in the xz plane. Thus, $(x_{i,n}',y_{i,n}',z_{i,n}')=(x_{i,n}\cos\theta-z_{i,n}\sin\theta,\ y_{i,n},\ z_{i,n}\cos\theta+x_{i,n}\sin\theta)$ = coordinates of the ith shared HCl electron or nth ion in a system of coordinates having its origin at the electrical center of HCl, z' axis coincident with $\mathbf{r}_{\text{Cl-H}}$ and y' axis coincident with the y axis.

The operator for the interaction energy between the two charge distributions is[15]

$$\begin{aligned}V=&-\frac{1}{R^3}\sum_{i,n;j}e_{i,n}e_j(2z_{i,n}z_j-x_{i,n}x_j-y_{i,n}y_j)\\&+\frac{3}{2R^4}\sum_{i,n;j}e_{i,n}e_j[r_{i,n}{}^2z_j-r_j{}^2z_{i,n}\\&+(2x_{i,n}x_j+2y_{i,n}y_j-3z_{i,n}z_j)(z_{i,n}-z_j)]+\cdots,\end{aligned}\quad(4)$$

where e_i and e_j represent the electronic charge, and $e_n=-e_i$. Neglecting in V all terms higher than dipole in the coordinates of the noble gas, Eq. (4) becomes

$$\begin{aligned}V\approx&-\frac{1}{R^3}\sum_{i,n;j}e_{i,n}e_j(2z_{i,n}z_j-x_{i,n}x_j-y_{i,n}y_j)\\&+\frac{3}{2R^4}\sum_{i,n;j}e_{i,n}e_j[r_{i,n}{}^2z_j\\&+z_{i,n}(2x_{i,n}x_j+2y_{i,n}y_j-3z_{i,n}z_j)]+\cdots,\end{aligned}\quad(5)$$

the first term representing the dipole-dipole and the second representing the dipole (noble gas) quadrupole (HCl) energy operators. The shift in ground-state eigenenergy for the interacting molecules is

$$\Delta E(R,\theta)=-\sum_{\lambda,k}{}'\frac{|\langle 00|V|k\lambda\rangle|^2}{E_{k0}+E_{\lambda 0}}\quad(6)$$

in second-order perturbation theory, where k and λ label the excited-electronic states of HCl and the noble gas, (00) representing the groundstate, and $(E_{k0}+E_{\lambda 0})$ is the difference in excited state (λk) and ground-state energies. The prime on the summation sign indicates that the sum is taken over all (λk) except (00).

[15] H. Margenau, Rev. Mod. Phys. **11**, 1 (1939).

Taking account of spherical symmetry in noble gases and cylindrical symmetry in HCl, and assuming that all $E_{\lambda 0}$ of importance can, to good approximation, be replaced by I_2 and all E_{k0} (except E_{00}) by I_1, where I_1 and I_2 are the ionization energies of HCl and the noble gas, one obtains for the R^{-6} terms

$$\Delta E(R^{-6}\text{ terms}) = -\frac{3}{2}\frac{I_1 I_2}{I_1+I_2}\alpha_2\left\{\left(\frac{\alpha_{11}+5\alpha_1}{6}\right)+\left(\frac{\alpha_{11}-\alpha_1}{2}\right)\cos^2\theta\right\}R^{-6} -\alpha_2\mu^2\{\tfrac{3}{2}\cos^2\theta+\tfrac{1}{2}\}R^{-6}, \quad (7)$$

which is identical to Eq. (1). Here, as is customary, we have made the identifications

$$\sum_n e_n \mathbf{r}_n = \mathfrak{y}, \quad (8)$$

$$\tfrac{2}{3}e^2\sum_\lambda |\langle 0|\sum_j r_j|\lambda\rangle|^2/E_{\lambda 0}=\alpha_2, \quad (9)$$

$$2e^2\sum_k |\langle 0|\sum_i z_i'|k\rangle|^2/E_{k0}=\alpha_{11}, \quad (10)$$

and

$$2e^2\sum_k |\langle 0|\sum_i x_i'|k\rangle|^2/E_{k0}=\alpha_1. \quad (11)$$

The R^{-7} terms in $\Delta E(R,\theta)$ are found by substituting Eq. (5) into Eq. (6) and selecting the appropriate terms, thus:

$$\Delta E(R^{-7}\text{ terms})\approx\frac{3\alpha_2 I_2}{R^7} \times\sum_k \frac{[\langle 0|\sum_{i,n} e_{i,n}z_{i,n}|k\rangle\langle k|\sum_{i,n}e_{i,n}(r^2-3z^2)_{i,n}|0\rangle-\langle 0|\sum_{i,n}e_{i,n}x_{i,n}|k\rangle\langle k|\sum_{i,n}e_{i,n}(xz)_{i,n}|0\rangle-(\text{etc. in } y)]}{E_{k0}+I_2}. \quad (12)$$

Here, again, we have employed Eq. (9). Now, whereas (x_n,y_n,z_n) and their powers have no finite off-diagonal elements, the diagonal elements of (x_i,y_i,z_i) vanish. Therefore, the sum over k in Eq. (12) splits into two parts, and, replacing all nonvanishing E_{k0} by I_1, we obtain

$$\sum_k = \frac{1}{I_2}[\langle 0|\sum_n e_n z_n|0\rangle\langle 0|\sum_{i,n}e_{i,n}(r^2-3z^2)_{i,n}|0\rangle -\langle 0|\sum_n e_n x_n|0\rangle\langle 0|\sum_{i,n}e_{i,n}(xz)_{i,n}|0\rangle] -\frac{2e^2}{I_1+I_2}\langle 0|\sum_i (z^3)_i|0\rangle. \quad (13)$$

Using the transformation relations

$$(x_{i,n},y_{i,n},z_{i,n})=(x_{i,n}'\cos\theta+z_{i,n}'\sin\theta, y_{i,n}', z_{i,n}'\cos\theta-x_{i,n}'\sin\theta), \quad (14)$$

$$\Delta E(R^{-7}\text{ terms})=-\frac{3\alpha_2\mu Q\cos^3\theta}{R^7} -\frac{6\alpha_2 e^2}{R^7}\frac{I_2}{I_1+I_2}[\langle 0|\sum_i (z'^3)_i|0\rangle\cos^2\theta +3\langle 0|\sum_i (x'^2z')_i|0\rangle\sin^2\theta]\cos\theta \quad (15)$$

is easily found. Here Q, simply called the quadrupole moment,[16] is

$$Q=\langle 0|\sum_{i,n} e_{i,n}(3z'^2-r^2)_{i,n}|0\rangle. \quad (16)$$

The approximate value of Q can be obtained from a knowledge of the r_n's, I_1, α_{11} and α_1. A simple calculation yields

$$Q\approx e[2\sum_n r_n^2-I_1(\alpha_{11}-\alpha_1)/e^2]=4.7\times 10^{-26}\text{ esu}. \quad (17)$$

The R^{-8} terms of $\Delta E(R,\theta)$ are similarly found. They are

$$\Delta E(R^{-8}\text{ terms})\approx -\frac{9\alpha_2 Q^2}{32R^8}(1-2\cos^2\theta+5\cos^4\theta). \quad (18)$$

We interpret the terms entering $\Delta E(R'\theta)$ in the following way. The terms in R^{-6} represent the usual London dispersion energy (written so as to account for the anisotropy of the HCl polarizability), along with the dipole-induced dipole energy. The terms in $\alpha_2\mu Q$ and $\alpha_2 Q^2$ represent quadrupole-induced dipole energies, where the inducing fields are those of the permanent dipole and quadrupole moments of HCl. The latter energy is not significant in broadening and will be neglected. The remaining R^{-7} terms are additional contributions to the dispersion energy, proportional to components of the electronic octupole moment tensor for the polar molecule. Although they are difficult to evaluate, for bound HCl these terms appear to be quite small; they vanish identically in cases where the diatomic molecule is electrically symmetric. We shall henceforth neglect them in our calculations. An approximate expression for the interaction between HCl and the noble gas is, therefore,

$$\Delta E(R,\theta)\approx -\frac{a_0}{R^6}-\frac{a_2}{R^6}\cos^2\theta-\frac{a_3 d}{R^7}\cos^3\theta, \quad (19)$$

[16] J. O. Hirschfelder, C. F. Curtiss, and R. B. Byrd, *Molecular Theory of Gases and Liquids* (John Wiley & Sons, Inc., New York, 1954).

with

$$a_0=\frac{3}{2}\frac{I_1I_2}{I_1+I_2}\alpha_2\left(\frac{\alpha_{11}+5\alpha_\perp}{6}\right)+\frac{\alpha_2\mu^2}{2}, \tag{20}$$

$$a_2=\frac{3}{2}\frac{I_1I_2}{I_1+I_2}\alpha_2\left(\frac{\alpha_{11}-\alpha_\perp}{2}\right)+\frac{3\alpha_2\mu^2}{2}, \tag{21}$$

and

$$a_3d=3\alpha_2\mu Q. \tag{22}$$

Finally, we express Eq. (19) in mass-center coordinates (R',θ'). Writing

$$\frac{1}{R}=\frac{1}{R'}\sum_{n=0}^{\infty}\left(\frac{d}{R'}\right)^n P_n(\cos\theta'), \tag{23}$$

where d is the distance separating the electrical and mass centers of HCl, and

$$\cos\theta=\cos\theta'-(d/R')\sin^2\theta' -\tfrac{3}{2}(d/R')^2\cos\theta'\sin^2\theta'+\cdots. \tag{24}$$

The most important contributions to $H_{\text{coll}}(1,2,;t)$ are

$$H_{\text{coll}}(1,2;t)\approx-(a_0+\tfrac{1}{3}a_2)R'(t)^{-6}-[6a_0+(14/5)a_2+(3/5)a_3]dP_1(\cos\theta')R'(t)^{-7} -(16(d/R'(t))^2a_0+(26/7)(d/R'(t))^2a_3+\tfrac{2}{3}a_2)P_2(\cos\theta')/R'(t)^{-6}. \tag{25}$$

Assuming that the Cl^+-ionic core is rigid and spherically symmetric, the electrical center is displaced from midway between H^+ and Cl^+ through distance $|\mu|/2|e|$ toward Cl^+, thereby producing the observed dipole moment. Accordingly, the distance between electrical and mass centers is

$$d=\tfrac{1}{2}r_e\left(1-\frac{|\mu|}{|e|r_e}-\frac{2m_{\text{H}}}{m_{\text{H}}+m_{\text{Cl}}}\right)=0.49\text{ Å}. \tag{26}$$

The interaction, Eq. (25), is still dominated by the isotropic dispersion force acting at distance d from the center of mass, inasmuch as Eq. (3) with d given by Eq. (26), constitutes a good approximation to Eq. (25).

The "eccentricity effect" (existence of finite d) exhibits itself not only in heteronuclear diatomic molecules, but shows a strong isotopic dependence in electrically homonuclear molecules. For example, in H_2, HD and HT, $d=0$, $\frac{1}{6}r_e$, and $\frac{1}{4}r_e$, respectively. For these molecules, Eq. (25) holds, with a_3 and μ both equal to zero.

The $P_2(\cos\theta')$ terms of $H_{\text{coll}}(1,2;t)$ have negligible influence on the line shapes,[17] so that Eq. (25) can be written, for purposes of calculation,

$$H_{\text{coll}}(1,2;t)\approx-\frac{C(v)}{R(t)^6}-\frac{6dC(0)(1+\delta)}{R(t)^7}P_1(\cos\theta), \tag{27}$$

dropping the primes on R and θ and neglecting the dependence of the $P_1(\cos\theta)$ terms on the vibrational quantum number. In Eq. (27)

$$C(v)=\frac{3}{2}\frac{I_1I_2}{I_1+I_2}\alpha_2\alpha_1(v), \tag{28}$$

with

$$\alpha_1(v)=\tfrac{1}{3}[\alpha_{11}(v)+2\alpha_\perp(v)] \tag{29}$$

and

$$\delta=\frac{1}{C(0)}\left\{\frac{4a_2+3a_3}{30}+\mu^2\alpha_2\right\}\approx0.11, \tag{30}$$

neglecting the slight variation in δ from one foreign gas to another. (The value given here is correct for argon.)

III. THEORETICAL

A. General

We shall elucidate the present theory where it differs from Anderson's,[13,14] a knowledge of that theory being assumed. We consider that the collisions which are critical in line broadening are those in which the emitter and perturber follow straight line paths with constant velocity. Three-body collisions, and in foreign-gas broadening, collisions between two HCl molecules (emitters) are assumed to be so infrequent as to have no practical importance, as is justified by the experimental situation.

For an ensemble of molecules in thermal equilibrium, the quantum mechanical Fourier integral formula[18] gives the intensity of net absorption of radiation per unit incident intensity at frequency ω in the form

$$I(\omega)\propto\omega\int_{-\infty}^{\infty}d\tau\,e^{-i\omega\tau}F(\tau), \tag{31}$$

where the correlation function, $F(\tau)$, is

$$F(\tau)=\langle\text{Tr}\{(\rho\mathfrak{y}(t)-\mathfrak{y}(t)\rho) \times\mathfrak{X}^{-1}(t\to t+\tau)\mathfrak{y}(t+\tau)\mathfrak{X}(t\to t+\tau)\}\rangle_t. \tag{32}$$

Here, $\mathfrak{X}$ and $\mathfrak{y}$ are the time development and electric dipole moment matrices in the adiabatic representation,

[17] R. M. Herman, thesis, Yale University, 1962 (unpublished).

[18] This formula has been derived in Ref. 14.

to be discussed shortly. The notation $\langle \mathrm{tr}\{\ \}\rangle_t$ indicates that the time (t) average of the trace is to be taken. The elements of the statistical matrix, ρ, for the molecular system are those corresponding to a Maxwell-Boltzmann distribution,

$$\rho_{jk} \propto e^{-E_j^0/kT}\delta_{j,k}\,, \tag{33}$$

E_j^0 being the energy which characterizes a pair of noninteracting molecules in a given bimolecular state, j. The symbols j, k, $\cdots$ refer to particular choices of quantum numbers which characterize the two molecules, and, as we assume both molecules to be in their electronic ground states, they actually denote specific choices of (vJM), the vibration, rotation, and magnetic quantum numbers which label the states of the vibrating rotator.

Equations (31) and (32) contain the information necessary to compute the entire spectrum of the ensemble. However, we are primarily concerned with single lines associated with radiative transitions which take molecules, say, in state $(v_iJ_iM_i)$ to state $(v_fJ_fM_f)$. In general, several values of the magnetic quantum numbers, M_i and M_f, are involved in each line. We are considering, here, well separated lines $(v_iJ_i \rightarrow v_fM_f)$ whose unperturbed center frequencies are denoted by ω_{fi}^0. Allowing i and f simply to label the vibration and rotation quantum numbers of the initial and final levels associated with the transition, it is customary[13] to write for the transition $(i \rightarrow f)$,

$$I_{(i\rightarrow f)}(\omega-\omega_{fi}^0) \propto (\rho_i-\rho_f)\omega \times\int_{-\infty}^{\infty} d\tau\, e^{-i(\omega-\omega_{fi}^0)\tau}F_{(if)}(\tau)\,, \tag{34}$$

where now

$$F_{(if)}(\tau)=\langle \mathrm{Tr}^{(if)}\{\mathfrak{y}(t)\mathfrak{X}^{-1}(t\rightarrow t+\tau) \times\mathfrak{y}(t+\tau)\mathfrak{X}(t\rightarrow t+\tau)\}\rangle_t e^{-i\omega_{fi}^0\tau}. \tag{35}$$

Here, we have used the abbreviation

$$\mathrm{Tr}^{(if)}\{ABCD\}\equiv \sum_{M_iM_fM_f'M_i'} A_{(i,M_i)(f,M_f)}B_{(f,M_f)(f,M_f')} \times C_{(f,M_f')(i,M_i')}D_{(i,M_i')(i,M_i)}. \tag{36}$$

As we have already mentioned, the matrices $\mathfrak{X}$ and $\mathfrak{y}$ are to be calculated in the adiabatic representation. We now discuss the basis functions for this representation, together with some properties of the time development matrix. Let us consider a set of "collision smeared" total molecular-state functions[19] for a given pair of interacting molecules, $\Phi_j(t+\tau)$, which obey the Schrödinger time equation

$$i\hbar\partial\Phi(t+\tau)/\partial\tau=H(t+\tau)\Phi(t+\tau)\,. \tag{37}$$

[19] S. Bloom and H. Margenau, Phys. Rev. **90**, 791 (1953).

In binary collisions, the total molecular Hamiltonian is

$$H(t)=H_0(1)+H_0(2)+H_{\mathrm{coll}}(1,2;t)\,, \tag{38}$$

where $H_0(1)$ and $H_0(2)$ are the Hamiltonians governing the isolated emitter (1) and perturber (2), and $H_{\mathrm{coll}}(1,2;t)$ is the collision Hamiltonain, expressed as a function of the internal coordinates of each and the separation between the centers of mass, which depends explicitly on time. We now expand the collision-smeared functions in terms of another set of time varying orthonormal functions, $\phi_k(t+\tau)$, thus:

$$\Phi_j(t+\tau)=\textstyle\sum_k \mathfrak{X}_{kj}(t\rightarrow t+\tau)\phi_k(t+\tau)\,. \tag{39}$$

The basis functions in the adiabatic representation, $\phi_k(t+\tau)$, are chosen so that at any instant of time they satisfy the stationary Schrödinger equation for the bimolecular system,

$$(H(t+\tau)-E_k(t+\tau))\phi_k(t+\tau)=0\,. \tag{40}$$

For convenience, we choose the time varying phases of $\phi_k(t+\tau)$ so that

$$\phi_k(t+\tau)=u_k(t+\tau)\exp\left[-i\hbar^{-1}\int^{t+\tau}E_k(t')dt'\right], \tag{41}$$

the phases of the $u_k(t+\tau)$, themselves, being constant in time. (The ϕ_k's are defined so that their axis of quantization coincides with the intermolecular axis. Because $H(t)$ is cylindrically symmetric about this axis [the $z'(t)$ axis],

$$[J_{z'(t)},H(t)]=0 \tag{42}$$

for all time. Equation (42) tells us that, in binary collisions, the component of angular momentum along the intermolecular axis associated with the eigenfunctions ϕ_k is always a good quantum number. Thus, although the ϕ_k are deformed by the interaction, they still rigorously obey many selection rules already obeyed by their simpler, undeformed counterparts.)

By substituting Eq. (39) into Eq. (37), with the aid of Eq. (40), the Schrödinger equation for $\mathfrak{X}$ is seen to be

$$i\hbar d\mathfrak{X}(t\rightarrow t+\tau)/d\tau=[H(t+\tau)-D]\mathfrak{X}(t\rightarrow t+\tau)\,, \tag{43}$$

where D stands for the operator $i\hbar\partial/\partial\tau$. We further impose the condition that at time $\tau=0$,

$$\Phi_j(t)=\phi_j(t)\,, \tag{44}$$

which is equivalent to the condition

$$\mathfrak{X}(t\rightarrow t)=\mathbf{1}\,. \tag{45}$$

At this point, through arguments similar to those employed by Anderson, a differential equation govern-

ing the behavior of $F_{(if)}(\tau)$ can be derived, and the resulting width and shift of the predicted Lorentz-type contour are obtained. We merely state the results here. Assuming that all collisions occur with velocity $\bar{v}$, the mean relative velocity between emitters and perturbers, the width at half intensity, and the shift in center frequency are

$$\text{width}=2n\bar{v}\,\text{Re}\{\sigma_{(if)}\}\,, \tag{46}$$

$$\text{shift}=-n\bar{v}\,\text{Im}\{\sigma_{(if)}\}\,, \tag{47}$$

where n is the numerical density of perturbers in the sample. The optical cross section in the adiabatic representation has a form analogous to that in the Heisenberg representation. Specifically,

$$\sigma_{(if)}=2\pi\int_0^\infty bdb\,S_{(if)}(b)\,, \tag{48}$$

where now the differential optical cross section is

$$S_{(if)}(b)=\left\{1-\frac{\text{Tr}^{(if)}\{\mathfrak{y}(0)\mathfrak{X}^{-1}(d\tau;b)\mathfrak{y}(d\tau;b)\mathfrak{X}(d\tau;b)\}e^{-i\omega_{fi}{}^0d\tau}}{\text{Tr}^{(if)}\{\mathfrak{y}(0)\mathfrak{y}(0)\}}\right\}. \tag{49}$$

Here, $\mathfrak{X}(d\tau;b)$ and $\mathfrak{y}(d\tau;b)$ represent those matrices after a time $d\tau$ in which one and only one collision, characterized by impact parameter b, has taken place.

B. Calculation of $S_{(if)}(b)$

We express the eigenstates, ϕ_k, in a coordinate system whose axis of quantization coincides with the intermolecular axis [the $z'(t)$ axis], and whose y axis coincides with the axis about which $z'(t)$ rotates during the collision. The Euler angles through which this coordinate system rotates during a collision, therefore, are (α,β,γ) with α and γ both zero and β running between 0 and π. This is illustrated in Fig. 2, where the primed system turns during the collision, the unprimed remaining stationary. In analyzing what happens during a collision, it is convenient to use the angle β as a parameter to indicate the extent to which it has progressed. For example, $\mathfrak{X}(\beta;b)$ is the $\mathfrak{X}$ matrix during a collision characterized by impact parameter b in which the intermolecular axis has rotated through the angle β. We therefore identify the matrices $\mathfrak{X}(d\tau;b)$ and $\mathfrak{y}(d\tau;b)$ in Eq. (49) with $\mathfrak{X}(\pi;b)$ and $\mathfrak{y}(\pi;b)$.

Now, for collisions whose impact parameters are very large, the identity

$$\lim_{b\to\infty}\{\mathfrak{X}^{-1}(\beta;b)\mathfrak{y}(\beta;b)\mathfrak{X}(\beta;b)\}_{(f,M_f)(i,M_i)}=\mathfrak{y}(0)_{(f,M_f)(i,M_i)}e^{i\omega_{fi}{}^0d\tau(\beta)} \tag{50}$$

holds, for no physical effect can result from infinitely distant collisions. Consequently, we identify $\mathfrak{X}(\beta;b=\infty)$ with the matrix of the inverse three-dimensional rotation operator, $R^{-1}(0,\beta,0)$, formed with the simple product (undeformed) eigenfunctions of the two molecules. Rose[20] has shown that the elements of these matrices, written as $d_{M'M}{}^J(-\beta)$, are finite only between states belonging to the same irreducible representation of the three-dimensional rotation group. Under the present circumstances, the $d^J(-\beta)$ matrices follow the time-development equation

$$i\hbar\dot{d}^J{}_{M'M}(-\beta)=-\dot{\beta}\sum_{M''}J_{y(JM')(JM'')}{}^{(b=\infty)}d^J{}_{M''M}(-\beta)\,, \tag{51}$$

where the matrix elements on J_y, the component of angular momentum along the y axis, are formed with the undeformed eigenfunctions in the rotating system. In view of Eq. (43), we arrive at the operator equation

$$(H-D)=-\dot{\beta}J_y\quad(b\to\infty)\,. \tag{52}$$

Our program for the calculation of $S_{(if)}(b)$ is this. We know, through standard intermolecular force calculations, how $\mathfrak{y}$ behaves during collisions. The problem is to compute $\mathfrak{X}(\pi;b)$ which, as we have seen, is approximately the inverse three-dimensional rotation matrix, and reduces to this in the limit of infinite impact parameter. We therefore seek the first- and second-order (in the collision Hamiltonian) corrections to this matrix for $b\neq\infty$. Then, on substituting the Taylor expansion of $\mathfrak{y}(\pi;b)$ and $\mathfrak{X}(\pi;b)$ into Eq. (49), we obtain the (first-three terms in the) Taylor series for $S_{(if)}(b)$.

There being no unique method for determining the corrections to the $\mathfrak{X}$ matrix, a procedure which seems optimal to the author is followed. We begin by defining a generalized rotation matrix, $\mathfrak{X}^J$ which satisfies the equation

$$i\hbar d\mathfrak{X}^J(\beta;b)/dt=(H-D)^J\mathfrak{X}^J(\beta;b)\,. \tag{53}$$

Here, $(H-D)^J$ has elements defined through the relations

$$(H-D)^J{}_{(j,M)(k,M')}=(H-D)_{(j,M)(j,M')}\delta_{j,k}\,. \tag{54}$$

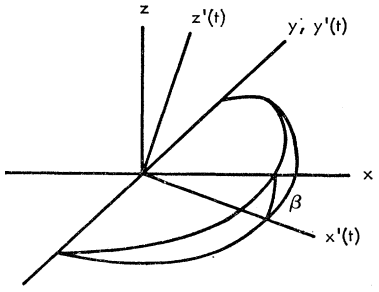

FIG. 2. Rotating and fixed coordinates.

[20] M. E. Rose, *Elementary Theory of Angular Momentum* (John Wiley & Sons, Inc., New York, 1957).

Consequently, $\mathfrak{A}^J$, like $d^J(-\beta)$, has finite elements only between initially degenerate states (hence the superscript "J"); and it reduces to the customary (inverse) rotation matrix in the limit $b\to\infty$. The $\mathfrak{A}^J$ matrix carries information regarding rotational adiabaticity in molecular collisions. Next, we introduce an inelastic scattering matrix, $\mathcal{T}$, through the relation,

$$\mathfrak{A}(\beta;b)=\mathfrak{A}^J(\beta;b)\mathcal{T}(\beta;b), \tag{55}$$

$\mathcal{T}$ remaining unity during impacts in which the inelastic scattering amplitudes remain zero. The function $S_{(if)}(b)$ can now be written

$$S_{(if)}(b)=\left\{1-\frac{\mathrm{Tr}^{(if)}\{\mathfrak{v}(0)\mathcal{T}^{-1}(\pi;b)\mathfrak{A}^{J-1}(\pi;b)\mathfrak{v}(\pi;b)\mathfrak{A}^J(\pi;b)\mathcal{T}(\pi;b)\}e^{-i\omega_{fi}{}^0 d\tau(\pi)}}{\mathrm{Tr}^{(if)}\{\mathfrak{v}(0)\mathfrak{v}(0)\}}\right\}, \tag{56}$$

the lower order contributions to $S_{(if)}(b)$ arising from the deviations of $\mathcal{T}$ and $\mathfrak{A}^J$ from unity and R^{-1}, and from the phase shifts associated with the time varying exponentials of the $\mathfrak{v}$-matrix elements.

There are two adiabatic limits of interest in collision-broadening problems.[21] In both of these, of course, inelastic collisions are absent. In adiabaticity of the first type, the collision-smeared states remain quantized in a space-fixed coordinate system. Here,

$$\mathfrak{A}^J(\beta;b)\approx R^{-1}(0,\beta,0),$$

as seen above. Adiabaticity of the second kind is characterized by the fact that collision-smeared states remain quantized in the rotating intermolecular system. In this case,

$$\mathfrak{A}^J(\beta;b)\approx\mathbf{1}.$$

This is more nearly the case for small b, where initially degenerate levels are well-split by the interaction. The transition between the two types of adiabaticity as a function of b, and the role of rotational effects (along with the associated phase shifts) in influencing line shapes has been examined in detail in Ref. 17. The conclusions reached are that, inasmuch as these effects, governed by the $P_2(\cos\theta)$ terms of $H_{\mathrm{coll}}(1,2;t)$, are influential in determining the line shapes, the Ben-Reuven, Friedman, and Jaffe[12] treatment is essentially correct. However, these effects play a minor role in HCl-line broadening. Instead, they are masked by the influence of the isotropic and $P_1(\cos\theta)$ terms of H_{coll}, which—in first order—do not lift degeneracies, but, rather, dominate the broadening through their influence on the $\mathfrak{v}$ and $\mathcal{T}$ matrices. Accordingly, replacing $\mathfrak{A}^J$ by $R^{-1}(0,\beta,0)$ and introducing $\eta_{fi}(b)$, the mean collisional phase-shift difference between states associated with the fth and ith levels,

$$\eta_{fi}(b)\equiv\hbar^{-1}\int_{\mathrm{coll}}dt\{\langle E_{(f,M_f)}(t;b)\rangle_{M_f}-\langle E_{(i,M_i)}(t;b)\rangle_{M_i}-\hbar\omega_{fi}{}^0\}, \tag{57}$$

$S_{(if)}(b)$ becomes

$$S_{(if)}(b)\approx\left\{1-\frac{\mathrm{Tr}^{(if)}\{\mathfrak{v}(0)\mathcal{T}^{-1}(\pi;b)\mathfrak{v}(0)\mathcal{T}(\pi;b)\}e^{i\eta_{fi}(b)}}{\mathrm{Tr}^{(if)}\{\mathfrak{v}(0)\mathfrak{v}(0)\}}\right\}. \tag{58}$$

The phase-shift approximation is valid if $\mathcal{T}(\pi;b)\approx\mathbf{1}$, in which case the familiar

$$S_{(if)}(b)\approx\{1-e^{i\eta_{fi}(b)}\} \tag{59}$$

results.

The differential equation governing $\mathcal{T}(\beta;b)$ is obtained by substituting Eq. (55) into Eq. (43). With the aid of Eq. (53), we find

$$i\hbar(d\mathcal{T}/dt)=\mathfrak{A}^{J-1}[(H-D)-(H-D)^J]\mathfrak{A}^J\mathcal{T}, \tag{60}$$

or simply

$$i\hbar(d\mathcal{T}/dt)=\mathfrak{A}^{J-1}(D^J-D)\mathfrak{A}^J\mathcal{T}. \tag{60a}$$

We then expand,

$$\mathcal{T}=\mathbf{1}+\sum_{n=1}^{\infty}\mathcal{T}^{(n)}, \tag{61}$$

$\mathcal{T}^{(n)}$ being governed by

$$i\hbar(d\mathcal{T}^{(n)}/dt)=\mathfrak{A}^{J-1}(D^J-D)\mathfrak{A}^J\mathcal{T}^{(n-1)}. \tag{62}$$

It is apparent from Eq. (62) that $\mathcal{T}^{(1)}$ cannot connect initially degenerate states. On the other hand, the $\mathcal{T}$ elements of importance in Eq. (58) are those which *do* connect such states. Accordingly, to obtain terms in $S_{(if)}(b)$ to second order, we replace $\mathcal{T}$ by $(1+\mathcal{T}^{(2)})$ in that equation. Expanding the exponential $e^{i\eta_{fi}(b)}$ in powers of η and applying selection rules obeyed by the $\mathfrak{v}$-matrix elements, we obtain

$$S_{(if)}(b)=-i\eta_{fi}(b)+\tfrac{1}{2}\eta_{fi}(b)^2-\langle\mathcal{T}_{(f,M_f)(f,M_f)}{}^{(2)-1}(\pi;b)\rangle_{M_f}-\langle\mathcal{T}_{(i,M_i)(i,M_i)}{}^{(2)}(\pi;b)\rangle_{M_i}+\cdots, \tag{63}$$

where the notation $\langle\ \rangle_M$ indicates that the average over M is to be taken. Expanding $S_{(if)}(b)$ in ascending powers of H_{coll},

$$S_{(if)}(b)=\sum_{n=0}^{\infty}S_{(if)}{}^{(n)}(b), \tag{64}$$

and making identification with the terms in Eq. (63),

$$S_{(if)}{}^{(0)}(b)=0, \tag{65a}$$

$$S_{(if)}{}^{(1)}(b)=-i\eta_{fi}{}^{(1)}(b), \tag{65b}$$

[21] H. Margenau and M. Lewis, Rev. Mod. Phys. **31**, 569 (1959).

and

$$S_{(if)}{}^{(2)}(b)=\tfrac{1}{2}\eta_{fi}{}^{(1)2}(b) -i\eta_{fi}{}^{(2)}(b)-\langle\mathcal{T}_{(f,M_f)(f,M_f)}{}^{(2)-1}(\pi;b)\rangle_{M_f} -\langle\mathcal{T}_{(i,M_i)(iM_i)}{}^{(2)}(\pi;b)\rangle_{M_i} \quad (65c)$$

are obtained, $\eta_{fi}{}^{(n)}(b)$ representing the phase-shift contributions arising from nth-order perturbations in energy.

C. Calculation of the Diagonal $\mathcal{T}^{(2)}(\pi;b)$ Elements

Before going further, we must evaluate the (D^J-D) matrix. This can be accomplished by differentiating Eq. (40) with respect to time, multiplying on the left by $\phi_j(t+\tau)$ and integrating over configuration space to obtain

$$(D^J-D)_{jk}=i\hbar\dot{H}(\beta;b)_{jk}/E_{jk}(\beta;b)\,, \quad \text{states } j \text{ and } k \text{ nondegenerate} \quad (66)$$
$$=0\,, \quad \text{states } j \text{ and } k \text{ degenerate}.$$

In seeking terms second order in $H_{\text{coll}}(1,2;t)$, it is permissible to neglect all but the lowest order terms in (D^J-D) and $\mathfrak{K}^J$. Applying the theory of finite rotations and substituting from Eq. (66), Eq. (60a) now becomes

$$\frac{d\mathcal{T}_{jk}(\beta;b)}{dt}\approx\sum_{l,E_{jl}{}^0\neq0}\frac{\dot{H}(\beta;b)_{jl}{}^{(\beta=0)}}{E_{jl}{}^0}\mathcal{T}_{lk}(\beta;b). \quad (67)$$

where the $\dot{H}(\beta;b)$ matrix elements, formed on eigenfunctions in the fixed system, are

$$\dot{H}(\beta;b)_{jl}{}^{(\beta=0)}=\langle\phi_j(0)^*|\dot{H}(\beta;b)|\phi_l(0)\rangle e^{i\omega_{jl}{}^0d\tau(\beta)}. \quad (68)$$

Thus,

$$\mathcal{T}_{jj}{}^{(2)}(\pi;b)=-\sum_{k,E_{kj}{}^0\neq0}E_{kj}{}^{0-2}\int_0^{d\tau(\pi)}dt'\,\dot{H}(t';b)_{jk}{}^{(\beta=0)} \times\int_0^{t'}dt''\,\dot{H}(t'';b)_{kj}{}^{(\beta=0)}, \quad (69)$$

accurate to terms in second order. Since $\mathcal{T}$ is unitary,

$$\mathcal{T}_{jj}{}^{(2)-1}=\mathcal{T}_{jj}{}^{(2)*}.$$

Now $\dot{H}(\beta;b)$ can be found from Eq. (27) through straightforward calculation, employing standard rules for transformations between spherical harmonics in coordinate systems rotated with respect to one another. Denoting by θ_0 and ϕ_0 the polar and azimuthal angles in the fixed system,

$$\dot{H}=\frac{\gamma\bar{v}b^2}{R(t)^{10}}\left\{\left[1-7\left(\frac{\bar{v}t}{b}\right)^2\right]Y_1{}^0(\theta_0\phi_0) +4\sqrt{2}\left(\frac{\bar{v}t}{b}\right)[Y_1{}^{-1}(\theta_0\phi_0)-Y_1{}^1(\theta_0\phi_0)]\right\} \quad (70)$$

holds for straight trajectories, with

$$\gamma=6(\tfrac{4}{3}\pi)^{1/2}dC(0)(1+\delta). \quad (71)$$

In Eq. (70), we have omitted isotropic terms, in view of the fact that their matrix elements in Eq. (69) vanish. Substituting Eq. (70) into Eq. (69), and neglecting terms for which $v\neq v'$,

$$\mathcal{T}_{(vJM)(vJM)}{}^{(2)}(\pi;b)=-\sum_{J'\neq J,M'}\left(\frac{\gamma}{E_{J'J}{}^0}\right)^2\Bigg\{32\bar{v}^4b^2(\langle JM|Y_1{}^{-1}-Y_1{}^1|J'M'\rangle^{(\beta=0)})^2\int_{-\infty}^{\infty}\frac{tdt\,e^{-i\omega_{J'J}{}^0t}}{R(t)^{10}}\int_{-\infty}^{t}\frac{t'dt'\,e^{i\omega_{J'J}{}^0t'}}{R(t')^{10}}$$
$$+\bar{v}^2b^2(\langle JM|Y_1{}^0|J'M'\rangle^{(\beta=0)})^2\int_{-\infty}^{\infty}\frac{\left(1-7\left(\frac{\bar{v}t}{b}\right)^2\right)dt\,e^{-i\omega_{J'J}{}^0t}}{R(t)^{10}}\int_{-\infty}^{t}\frac{\left(1-7\left(\frac{\bar{v}t'}{b}\right)^2\right)dt'\,e^{i\omega_{J'J}{}^0t'}}{R(t')^{10}}\Bigg\} \quad (72)$$

is obtained. The averages over M in Eq. (65c) can be taken with the summation on M' in Eq. (72). For rigid rotator eigenfunctions,

$$\langle\mathcal{T}_{(vJM)(vJM)}{}^{(2)}(\pi;b)\rangle_M =-\sum_{J'}\left(\frac{\gamma}{E_{J'J}{}^0}\right)^2\frac{g(J,J')A(k_{J'J})}{b^{14}} \quad (73)$$

is obtained, with

$$A(k)=64\int_{-\infty}^{\infty}\frac{xdx\,e^{-ikx}}{(1+x^2)^5}\int_{-\infty}^{x}\frac{x'dx'\,e^{ikx'}}{(1+x'^2)^5} +\int_{-\infty}^{\infty}\frac{(1-7x^2)e^{-ikx}dx}{(1+x^2)^5}\int_{-\infty}^{x}\frac{(1-7x'^2)e^{ikx'}dx'}{(1+x'^2)^5} \quad (74)$$

and

$$g(J,J')=\frac{1}{4\pi(2J+1)}(J\delta_{J,J'+1}+(J+1)\delta_{J,J'-1}). \quad (75)$$

Here, we have introduced the variables

$$x=\bar{v}t/b \quad \text{and} \quad k_{J'J}=\omega_{J'J}{}^0 b/\bar{v}.$$

The function $A(k)$, equal to $A^*(-k)$, has been evaluated[17] by replacing $(1+x^2)^{-5}$ by $e^{-(2.06x)^2}$ in Eq. (74). The replacement function, very similar in appearance to the original, has been normalized with respect to its value at $x=0$ and its integral over x from $-\infty$ to ∞. The accuracy to which $A(k)$ is obtained in this approximation is indicated in part by the fact that $\int_{-\infty}^{\infty} A(k)dk$, when calculated approximately, differs from the exact value by 2.4%. The function $A(k)$, together with its asymptotic value,

$$\lim_{k\to\infty} A(k)=-i2.705/k, \quad (76)$$

is shown in Fig. 3.

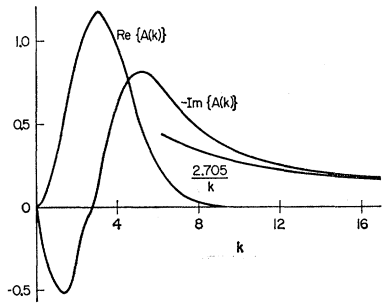

FIG. 3. The function $A(k)$.

D. Further Reduction of $S_{(if)}(b)$

It remains now for us to calculate the first and second order phase shifts appearing in $S_{(if)}{}^{(1)}(b)$ and $S_{(if)}{}^{(2)}(b)$. For the former, only the first term in Eq. (27) is important. For R^{-6}-dependent perturbations,[21]

$$\eta_{fi}{}^{(1)}(b)=-\frac{3\pi C(0)}{8\hbar\bar{v}b^5}\left(\frac{\alpha_1(v_f)-\alpha_1(v_i)}{\alpha_1(v_i)}\right) \quad (77)$$

independent of rotational quantum number.

The second-order phase shifts vanish for all but the R_0 and P_1 lines, consequent to the fact that second-order perturbations, when averaged over M, vanish for all but the $J=0$ levels. This phase shift, for these levels, is

$$\eta_{J=0}{}^{(2)}(b)=-\frac{231}{4096}\left(\frac{\gamma}{E_{10}{}^0}\right)^2\frac{k_{10}}{b^{14}}, \quad (78)$$

as can be easily verified. The fact that

$$\int_{-\infty}^{\infty}\frac{dt}{R(t)^{14}}=\frac{231\pi}{1024\bar{v}b^{13}}$$

is useful in this connection.

Substituting Eqs. (73), (77), and (78) into (65b) and (65c), we obtain the following expressions for $S_{(if)}{}^{(1)}(b)$ and $S_{(if)}{}^{(2)}(b)$:

$$S_{(if)}{}^{(1)}(b)=-i\frac{3\pi C(0)}{8\hbar\bar{v}b^5}\left(\frac{\alpha_1(v_f)-\alpha_1(v_i)}{\alpha_1(v_i)}\right) \quad (79)$$

and

$$S_{(if)}{}^{(2)}(b)$$

$$=-\tfrac{1}{2}[S_{(if)}{}^{(1)}(b)]^2+\frac{48\pi d^2C(0)^2(1+\delta)^2}{b^{14}}$$

$$\times\left[\sum_{J'}\left(\frac{g(J_i,J')A(k_{J'J_i}(b))}{E_{J'J_i}{}^2}+\frac{g(J_f,J')A(k_{J_fJ'}(b))}{E_{J_fJ'}{}^2}\right)\right.$$

$$\left.+0.0562i\frac{k_{10}(b)}{E_{10}{}^2}(\delta_{J_f,0}-\delta_{J_i,0})\right]. \quad (80)$$

Inspection of Eq. (80) reveals that $S_{(if)}{}^{(2)}(b)$ is complex. This differs from the results of Anderson's theory, in which this quantity is real. The two treatments yield numerically equivalent forms for $S^{(2)}$ if one does not (as is usually done) neglect the noncommuting contributions to Anderson's time development matrices. The fact that $S^{(2)}$ is complex leads to differing shifts for the R and P branch lines of equal $|m|$, as are observed experimentally.

The terms to second order in the expansion of $S_{(if)}(b)$ constitute a good approximation to it for large impact parameters. On the other hand, for small values of b, this approximation is inadequate. Instead, we rely on physical arguments to tell us that very close collisions cause a complete interruption of the radiation, so that, effectively,

$$\lim_{b\to 0} S_{(if)}(b)=1.$$

We shall employ a method of approximating $S_{(if)}(b)$ for intermediate values of b, similar to that adopted by Tsao and Curnutte[14] (Anderson's approximation number two). In that treatment, $S_{(if)}(b)$ is identified with the first three terms of its series expansion for values of $b>b_0$, and is taken to be unity for $b<b_0$. The critical impact parameter, b_0, is determined through the condition

$$S_{(if)}{}^{(2)}(b_0)=1. \quad (81)$$

The logic here is that $S_{(if)}{}^{(3)}(b)$, $S_{(if)}{}^{(4)}(b)$, $\cdots$cannot be neglected when $S_{(if)}{}^{(2)}(b)\gtrsim 1$; hence, $S_{(if)}(b)$, for $b<b_0$, is thought to more nearly equal the "complete interruption" value of unity. Now, in our treatment, the situation is complicated by the fact that $S_{(if)}{}^{(2)}(b)$

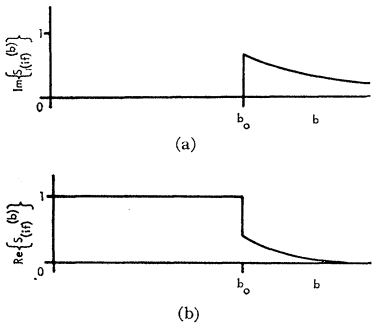

FIG. 4. Real and imaginary parts of $S_{(if)}(b)$ (schematic).

is complex. Moreover, the imaginary contributions to Eq. (65c) sometimes cancel, so that the $\mathcal{T}^{(2)}$ elements themselves might be quite small, even though $\mathcal{T}$ is not well approximated by its first three terms. Correspondingly, $S_{(if)}{}^{(3)}(b)$, $S_{(if)}{}^{(4)}(b)$, $\cdots$can be large, even though $S_{(if)}{}^{(2)}(b)$ is itself quite small. Consequently, a better criterion for determining b_0 is one on the magnitudes of the individual contributions to the $\mathcal{T}^{(2)}$ matrix elements. Our generalization of Eq. (81) as a condition on b_0 is, therefore, that the sum of the magnitudes of the individual contributions to $S_{(if)}{}^{(2)}(b)$ be unity, or, in our case,

$$-\tfrac{1}{2}[S_{(if)}{}^{(1)}(b_0)]^2+\frac{48\pi d^2C(0)^2(1+\delta)^2}{b_0{}^{14}}\times\Bigg[\sum_{J'}\Bigg(\frac{g(J_i,J')\,|A(k_{J'J_i}(b_0))|}{E_{J'J_i}{}^2}+\frac{g(J_f,J')\,|A(k_{J_fJ'}(b_0))|}{E_{J_fJ'}{}^2}\Bigg)+0.0562\frac{k_{10}(b_0)}{E_{10}{}^2}(\delta_{J_f,0}+\delta_{J_i,0})\Bigg]=1. \quad (82)$$

This condition reduces to Eq. (81) whenever all contributions to $S_{(if)}{}^{(2)}(b)$ are real. The real and imaginary parts of the $S_{(if)}(b)$'s resulting from our method of approximation are illustrated schematically below (Fig. 4).

Confining our attention to a single vibrational band, for the moment, we observe from Eqs. (79), (80), and (82) that

$$S_m{}^{(1)}(b)=S_{-m}{}^{(1)}(b), \quad (83)$$
$$S_m{}^{(2)}(b)=S_{-m}{}^{(2)*}(b),$$

and

$$(b_0)_m=(b_0)_{-m},$$

in view of the similarity in rotational structure of each vibrational level. These properties of $S_{(if)}(b)$ and b_0 imply, for the predicted widths and shifts, the following regularities:

TABLE I. The parameters α, I, and $C(0)$.

Gas	α (Å^3)	I (eV)	$C(0)\times10^{60}$ (erg cm^6)
HCl	2.64	13.8	...
He	0.205	24.5	11.5
Ne	0.39	21.5	20.8
Ar	1.63	15.7	75.9
Kr	2.46	13.9	108.0
Xe	4.01	12.1	164.5

(1) The widths of the m and $-m$ lines are equal within a given band.

(2) The shifts receive contributions from two terms, $S_{(if)}{}^{(1)}(b)$ and $\mathrm{Im}\{S_{(if)}{}^{(2)}(b)\}$. The contribution from $S_{(if)}{}^{(1)}(b)$ is the same, whereas that from $\mathrm{Im}\{S_{(if)}{}^{(2)}(b)\}$ has equal magnitude but opposite sign for the m and $-m$ lines.

(3) The mean (red) shift of the equal $|m|$ lines arises solely from $S_{(if)}{}^{(1)}(b)$, and varies, from one value of $|m|$ to another, as $b_0{}^{-3}$. The width of these lines, on the other hand, is proportional, roughly, to $b_0{}^2$. Therefore, an approximate relationship,

$$[\mathrm{shift}(m)+\mathrm{shift}(-m)]\times[\mathrm{width}(m)+\mathrm{width}(-m)]^{3/2}\approx\mathrm{const} \quad (84)$$

should hold.

Qualitatively, the gross features of noble-gas broadening can be understood in the following way. As J increases, spacings between adjacent energy levels also increase, with inelastic collisions becoming less frequent. Consequently, the higher $|m|$ lines are less severely broadened, as has been observed in experiment. Along with the decrease in width (and in b_0), the domain over which first-order phase shifts are to be integrated increases, increasing the mean red shift of the equal $|m|$ lines (unless, of course, short-range forces reverse this tendency for smaller b values). The tendency for the R and P branch lines of equal $|m|$ to shift unequally is most pronounced for the case $|m|=1$, inasmuch as second-order perturbations contribute to the phase shifts for these lines alone.

IV. RESULTS AND DISCUSSION

The numerical calculation of the widths and shifts is carried out using Eqs. (79) and (80) for $S_{(if)}{}^{(1)}(b)$ and $S_{(if)}{}^{(2)}(b)$, with $A(k)$ and $g(J,J')$ given by Eqs. (74) and (75), the condition Eq. (82) being used to determine b_0. The widths and shifts are then related to $S_{(if)}(b)$

TABLE II. The factors $[\alpha_1(v)-\alpha_1(0)]/\alpha_1(0)$.

v	(Ref. 7)	(Ref. 11)	(This paper)	$\alpha_1(v)$ (Å^3) (this paper)
0	0	0	0	2.64
1	0.011	0.019	0.025	2.71
2	0.025	$\approx$0.038	0.050	2.77

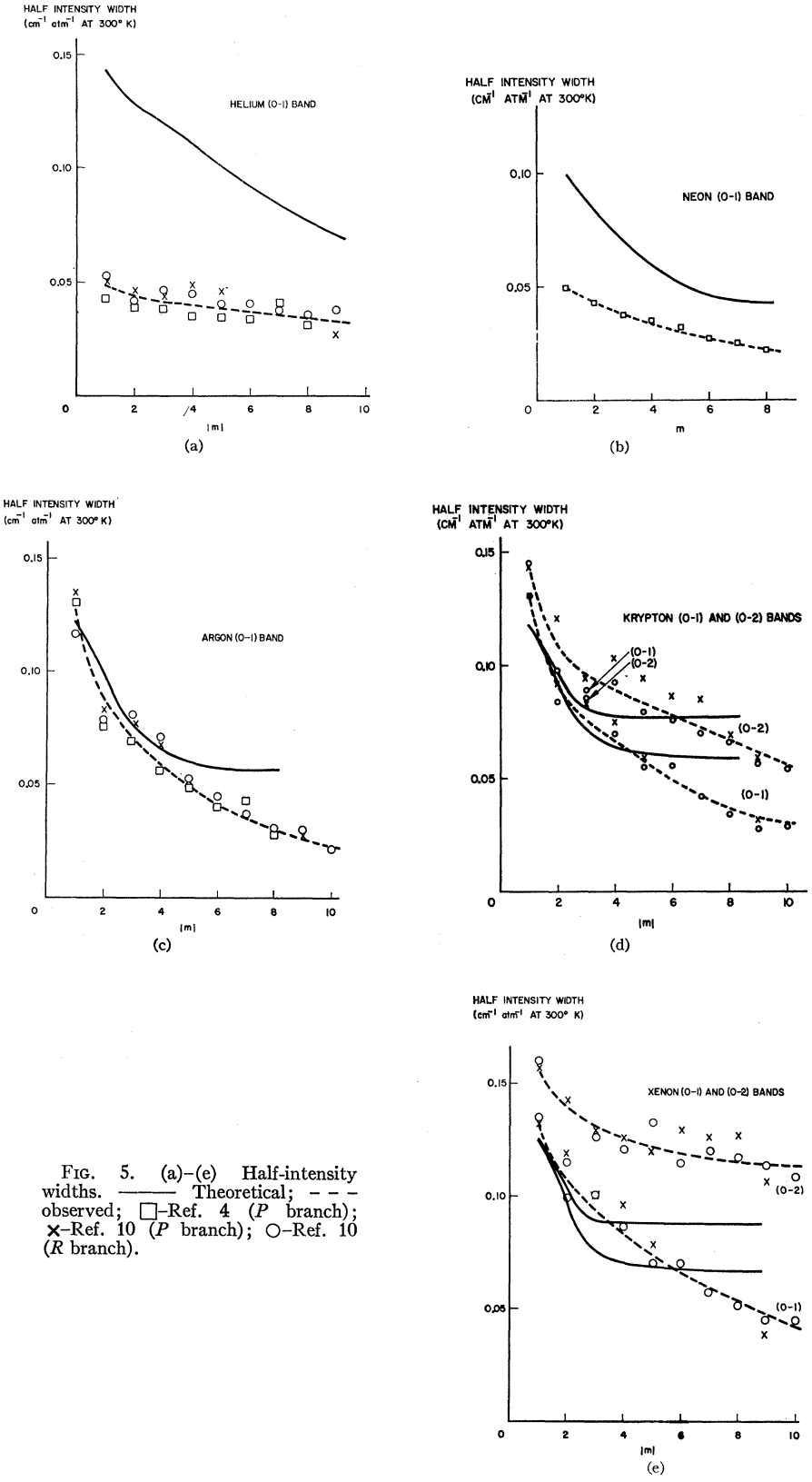

FIG. 5. (a)–(e) Half-intensity widths. ——— Theoretical; – – – observed; □–Ref. 4 (*P* branch); ×–Ref. 10 (*P* branch); ○–Ref. 10 (*R* branch).

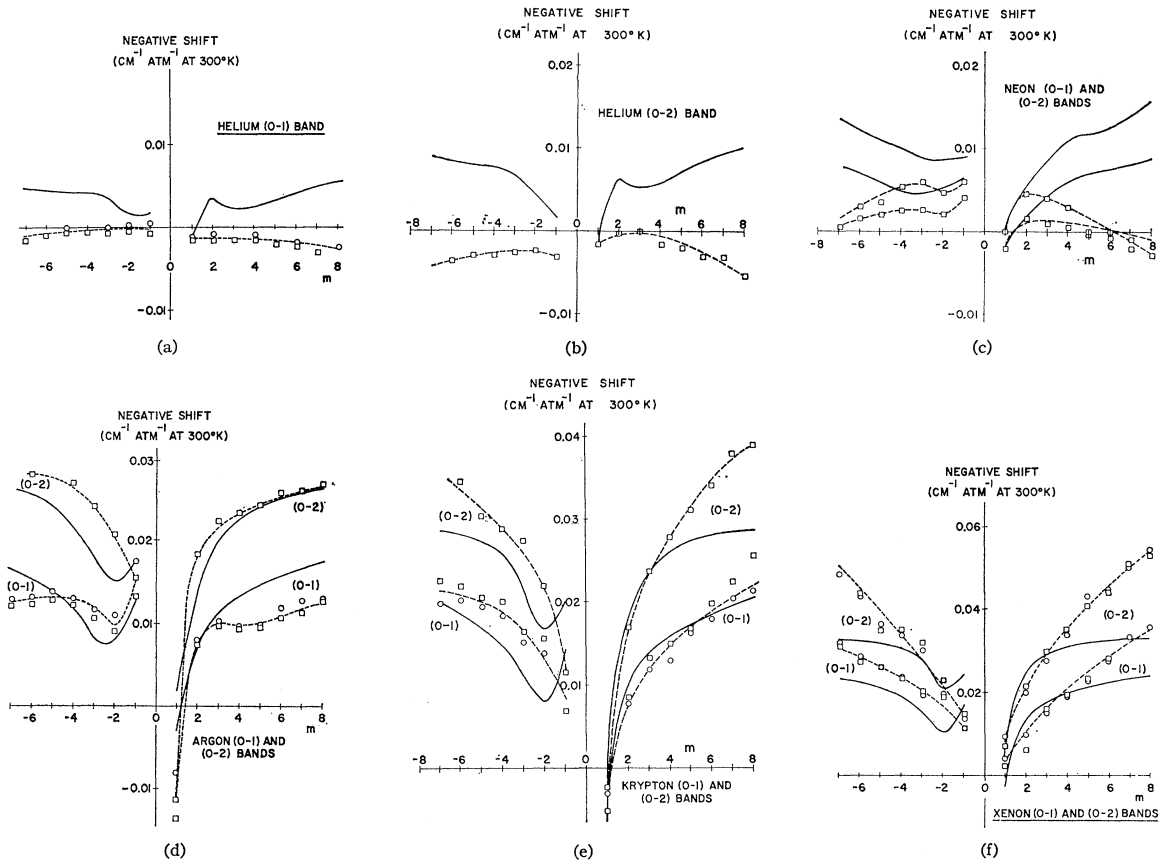

FIG. 6. (a)–(f) Negative line shifts. ——— Theoretical; – – – observed; □–Ref. 7; ○–Ref. 10.

through Eqs. (46), (47), and (48). Numerical values of the parameters α, I, and $C(0)$ needed for the calculation are given in Table I, while numerical values of the factor $[\alpha_1(v)-\alpha_1(0)]/\alpha_1(0)$ for $v=1$, 2 used in the calculation are given in Table II, together with the values of that parameter calculated by Ben-Reuven *et al.*[7] and by Schuller and Oksengorn.[11] Our values were chosen so as to fit the observed argon, krypton, and xenon induced low $|m|$ line shifts. The calculated widths and shifts are not very sensitive to small variations in this parameter, however.

The calculated values are indicated by solid lines in Figs. 5 and 6, along with experimental points through which broken lines have been drawn. In general, the agreement between our predictions and experiment is good. The volume and complexity of data to be explained, together with the over-all agreement, support the belief that we are basically correct in our description of noble-gas broadening. The most serious discrepancy lies in the variation in the magnitude of the widths in going from one broadener to another. The smallness of the He- and Ne-induced widths is indeed mystifying. Not only are the b_0 as inferred from these widths less than that impact parameter at which the adiabatic approximation is supposed to have broken down, but they are considerably less than the gas kinetic radii, as well. Because the experimental widths for He and Ne (also, higher $|m|$ line widths for heavier perturbers) are small, we expect short range forces[22] to be operative in determining the shifts of these lines. Consequently, it does not surprise us to find that some lines are blue shifted (with He), and as the widths become smaller we look for the lines to be shifted even more toward the blue, a fact that is observed experimentally.[23]

A less serious discrepancy lies in the fact that in Ar, Kr, and Xe broadening, the theoretical widths and shifts show a stronger tendency to level off then do their experimental counterparts. In our calculation, the leveling takes place when the phase shift terms in $S_{(if)}{}^{(2)}(b)$ become dominant over the inelastic collision terms. The leveling seems to be present in some of the observed widths [cf., xenon (0–2) band]; however, it has much less importance in practice than it does in theory. Here

[22] Because the HCl molecule effectively is more extended at higher v (consequent to the fact that the nuclei oscillate more widely about their equilibrium position), colliding molecules experience repulsive (exchange) forces at larger separations, the higher the HCl vibrational quantum number. Hence, short-range forces tend to widen the spacing of vibrational bands, causing blue shifting.

[23] Our remarks on the influence of short-range forces generally concur with those of the authors of Ref. 12.

again, exchange forces could act to prevent the observed widths and shifts from leveling off.

The observed

$$[\text{shift}(m)+\text{shift}(-m)][\text{width}(m)+\text{width}(-m)]^{3/2}$$

values, instead of being constant as theory predicts, increase then decrease as $|m|$ increases.[17,24] There is no obvious reason for the increase at low $|m|$. The decrease often occurs when the optical radii—as determined from the observed widths—approach or became smaller than the gas-kinetic radii. In He and Ne broadening, however, such a correlation cannot be found, all emperical optical radii being smaller than gas-kinetic from the start.

[24] R. M. Herman (to be published).

An experimental determination of the rare-gas-broadened pure rotation [(0–0) band] linewidths and shifts would be worthwhile at the present time. Since first-order phase shifting is not operative in broadening and shifting these lines, the effects of inelastic processes alone could be studied. To extend our calculations to these lines would be routine. However, this step has not yet been taken, inasmuch as comparison with experiment is impossible at the present time.

ACKNOWLEDGMENT

The author wishes to thank Professor Henry Margenau for calling attention to the line-shift problem and for continued helpful guidance throughout the course of this research.

PHYSICAL REVIEW VOLUME 132, NUMBER 1 1 OCTOBER 1963

Hyperfine Structure of Hg^{197} and Hg^{199}†

CARL V. STAGER*

Department of Physics and Research Laboratory of Electronics, Massachusetts Institute of Technology, Cambridge, Massachusetts

(Received 7 May 1963)

The hyperfine structure of the $^3P_1$ state of Hg^{197} and Hg^{199} has been measured by a microwave-optical experiment. This involves optical excitation to the desired state, paramagnetic resonance in this state, and an optical method of detecting the paramagnetic resonance. The paramagnetic resonances were obtained between different F levels as a function of magnetic field. Quadratic Zeeman corrections were estimated by second-order perturbation theory and the corrected transition frequencies were then extrapolated to zero field. The zero-field hyperfine-structure splittings in the $^3P_1$ state are $Hg^{197}(F=\frac{3}{2}$ to $F=\frac{1}{2})=23\,086.37(2)$ Mc/sec, $Hg^{199}(F=\frac{3}{2}$ to $F=\frac{1}{2})=22\,128.56(2)$ Mc/sec. Hyperfine-structure constants A are obtained which are correct to second order. These are combined with the known nuclear magnetic moments to give the hyperfine-structure anomaly in the $^3P_1$ state: $\Delta(^3P_1,Hg^{199},Hg^{201})=-0.00147(1)$, and the anomaly of the hyperfine-structure interaction for the $6s$ electron in the $^3P_1$ state: $\Delta(s_{1/2},Hg^{199},Hg^{201})=-0.00175(9)$.

I. INTRODUCTION

MERCURY has two stable isotopes with nonzero spin, Hg^{199} with $I=\frac{1}{2}$ and Hg^{201} with $I=\frac{3}{2}$. Hg^{197} is radioactive with a half-life of 65 h. It also has $I=\frac{1}{2}$. The hyperfine structure of the $^3P_1$ state of Hg^{201} has been measured by Kohler.[1] This work is basically an extension of Kohler's method, applied to Hg^{197} and Hg^{199}. The hyperfine-structure splittings in the $^3P_1$ state of Hg^{197} and Hg^{199} have been measured to an accuracy of approximately one part in a million. For both isotopes this represents an increase in the accuracy, over existing measurements, of a factor of approximately 100.

This increase in accuracy permits one to obtain the hyperfine-structure anomaly in the $^3P_1$ state. The hyperfine-structure anomaly for Hg^{199} and Hg^{201} has previously been measured in the $^3P_2$ state[2] and by means of the Knight shift.[3] The agreement between these results is excellent.

II. APPARATUS AND METHOD

A. Excitation and Detection

The relevant energy levels of the mercury atom are shown in Fig. 1. The $^3P_1$ state is connected to the $^1S_0$ ground state by the 2537 Å resonance line. On the right-hand side of Fig. 1, the relative positions of the hyperfine components of the 2537 Å line are shown, including only those isotopes that are relevant for this discussion.

† This work, which is based on a thesis submitted to the Department of Physics, Massachusetts Institute of Technology, in partial fulfillment of the requirements for the degree of Doctor of Philosophy, was supported in part by the U. S. Army, the Air Force Office of Scientific Research, and the Office of Naval Research.

* Present address: McMaster University, Hamilton, Ontario, Canada.

[1] R. H. Kohler, Phys. Rev. **121**, 1104 (1961).

[2] M. N. McDermott and W. L. Lichten, Phys. Rev. **119**, 134 (1960).

[3] J. Eisinger, W. Blumberg, and R. Schulman, Bull. Am. Phys. Soc. **4**, 451 (1959).